

# PASSIVE ACOUSTIC MONITORING OF OCEAN WEATHER PATTERNS

M. Keogh      Department of Physics, University of Bath, Bath BA2 7AY, UK  
Ph. Blondel    Department of Physics, University of Bath, Bath BA2 7AY, UK

## 1 INTRODUCTION

Ocean weather patterns (e.g. rainfall, wind, monsoon) are important contributors to Global Climate Models, in particular in the context of climate change. They can be measured, to some extent, by satellite remote sensing, but this is only achievable over large spatial scales, over finite time windows and in the satellite's field of view. Areas with sparse satellite coverage or lower spatial/temporal resolution, like the Arctic and Antarctic, are under-represented in these models despite their important contributions. Fortunately, ocean weather patterns can also be detected underwater by measuring their acoustic characteristics. This is particularly interesting as moored or drifting platforms can monitor the background noise of the ocean and access the time and space scales inaccessible to satellite or ship measurements. Our work aims at complementing existing models and observations with laboratory and field experiments of simple weather-related events.

The first dataset consists of field measurements conducted in the Arctic in summer 2007, along the fjord of Kongsfjord (Svalbard) and in proximity of the Ny-Ålesund international research station. They were taken with a broadband hydrophone (100 Hz – 48 kHz effective bandwidth), deployed 10-m deep at regular intervals in deep water from the mouth of the fjord toward the glaciers at its end. These measurements include varying ambient noise from wind and small waves, light rain, marine mammals and different types of growlers and bergy bits. The Arctic data is complemented with a second dataset acquired in the University of Bath tank facilities, using the same broadband hydrophone. These experiments include different types of rain (from single drops, of varying sizes, to intense rain), different wind speeds and different mimics of small growlers (with varying gas inclusions and melting rates).

The interpretation of these measurements is supported by several decades of research into ambient noise underwater<sup>1-5</sup>. Although the acoustic implications of individual physical events, like raindrops or wind, are now well understood, their characteristic acoustic signatures are still subject to debate<sup>3</sup>, particularly when several processes occur concurrently or when specific processing techniques are applied in new areas. This article is the first step of a work in progress. It intends to show the complementarities of tank experiments with real-world measurements, in terms of understanding individual and combined processes. And it presents a rigorous framework for analysing unknown field measurements of ambient noise, as suggested by Black et al.<sup>5</sup>, using Principal-Component Analyses (PCA) to identify ocean weather processes and their main frequency characteristics.

## 2 FIELD MEASUREMENTS IN THE ARCTIC

Kongsfjorden is an Arctic fjord on the NW coast of Spitsbergen (Svalbard). With neighbouring Krossfjorden, it forms a two-armed fjord system sharing a common mouth (Figure 1). Kongsfjorden is about 20 km long and 4-10 km wide. Acoustic mapping and sampling<sup>6</sup> show bedrock with relict sub-glacial, ice-scoured topography, overlaid by a thin (<10 m) sediment cover. Depths gradually decrease from 360 m in the outer basin to 60 m in the inner basin, separated by a 30-m deep ridge. Some deeper (~ 400 m) depressions also occur in the middle of the fjord. The outer zone of Kongsfjorden connects with Krossfjorden to form a submarine glacial trough, the Kongsfjordrenna,

which acts as a deep-water connection across the shelf<sup>7</sup>. This combination of geographical features makes for a complex oceanography along the fjord. Five tidewater glaciers drain into its inner zone, providing a major source of freshwater. With run-off (glacier ablation, snowmelt, summer rainfall and ice calving) and groundwater discharge, this forms 5% of the mass balance in the fjord<sup>7</sup>. At its mouth, the West-Spitsbergen Current (a branch of the North Atlantic Current) carries relatively warm and saline (>35 p.s.u) water along the coast. Arctic and Atlantic water masses advected from the shelf create significant temperature and salinity changes. Because of this combined influence, the fjord mixes boreal and Arctic ecosystems<sup>8</sup>. Kongsfjorden is an important feeding ground for marine mammals (including whales and seals) and seabirds.

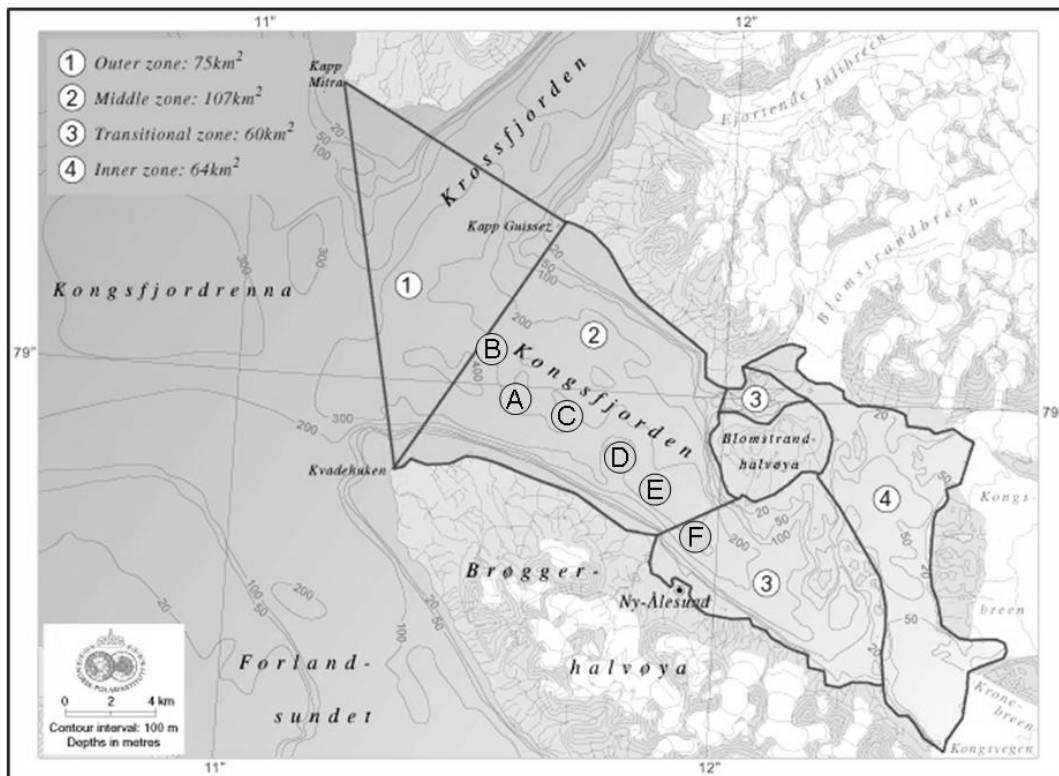


Figure 1: Map of Kongsfjord with positions of recording stations (circled letters). See Table 1 for details. Basemap from Norwegian Polar Institute (<http://miljo.npolar.no/temakart>).

Ambient noise was measured with a single hydrophone SQ26-07 (manufactured by Cetacean Research Technology, Seattle, USA). This hydrophone is omnidirectional at all frequencies considered, as confirmed by earlier tank tests. Its operational frequency band ranges from 10 Hz to 50 kHz, but sensitivity varies slightly throughout. It is nearly constant at -168 dB re. 1V/μPa from 100 Hz to 30 kHz, decreases linearly to -174 dB re. 1V/μPa at 35 kHz, and increases again to -168 dB re. 1V/μPa above 40 kHz. The preamplifier gain was fixed at 25 dB. The shielded cable length of 10 m, combined with low gunwale of the supporting vessel (a Buster-L boat with aluminium hull), allowed deployment to ~9.5 m depth each time. Data from the hydrophone was input in a digital recorder M-Audio Microtrack 24/96 (sampling at a frequency of 96 kHz). Measurements covered an effective broadband frequency range of 10 Hz to 48 kHz. They were acquired in water always deeper than 200 m and in several distinct environments (junction of Kongsfjorden with Krossfjorden, throughout the middle zone and close to the harbour) (Figure 1 and Table 1). The wind speed was measured as 11 km/h (Sea State 2) at the meteorological station in Ny-Ålesund; it is a lower estimate of that in the fjord and matches visual observations. Wind chill temperatures (an important parameter in ice melting) always remained sub-freezing. The different acoustic measurements are recorded in 24-bit .WAV format, ensuring full access to the normalised waveform.

<b>Position A</b> – 78°59'45.7"N ; 11°34'47.4"E – File A (5'00") Light rain. Small waves. No ice. Depth ~ 300 m – Closest shore ~ 3 km away. Whale less than 50 m away + distant ship (~ 5 km)
<b>Position B</b> – 79°00'53.6"N ; 11°30'00.4"E – Files B <sub>1</sub> (1'20"), B <sub>2</sub> (2'01"), B <sub>3</sub> (3'01") Light rain. Very small waves. No ice. Depth ~ 300 m – Closest shore ~ 4 km away. Whale visible at the surface + ship at horizon (> 5 km)
<b>Position C</b> – 78°59'30.9"N ; 11°40'41.8"E – Files C <sub>1</sub> (0'46"), C <sub>2</sub> (3'01"), C <sub>3</sub> (3'01") Light rain, increasing. No waves. No ice. Depth ~ 300 m – Closest shore ~ 3 km away.
<b>Position D</b> – 78°58'47.4"N ; 11°46'53.4"E – Files D <sub>1</sub> (3'00"), D <sub>2</sub> (1'31") No rain. No waves. No ice. Depth ~ 300 m – Closest shore ~ 2 km away.
<b>Position E</b> – 78°58'01.0"N ; 11°52'26.9"E – File E (2'01") Very light rain. Very small swell. Small icebergs (growlers and bergy bits) ~20 m away. Depth ~ 250 m – Closest shore ~ 1.9 km
<b>Position F</b> – 78°57'09.4"N ; 11°57'42.2"E – File F (2'00") No rain. No waves. No ice. Depth ~ 200 m – Closest shore ~ 1.9 km away In front of Ny-Ålesund harbour, with cruise ship at berth.

Table 1. Details of measurements at each recording station, including duration. Several recordings were taken at stations B, C and D to measure ambient noise stationarity.

### 3 ANALYSIS OF THE ARCTIC DATASET

The time-domain measurements vary significantly with location (Figure 2). Their differences are even more visible in the frequency domain. For analysis, each recording was divided into 8,192-point segments (i.e. ~ 85 ms at the sampling rate used), a duration commensurate with those used in the literature<sup>5</sup>. The segments overlapped by 10%, to prevent cutting off processes of interest. The FFT of each segment was calculated in Matlab and the values of the power spectra were averaged over frequency ranges of 1 kHz, between 1 and 48 kHz.

Average powers at specific frequencies can be used as acoustic discriminants, as successfully shown by other workers<sup>4,5</sup>. Frequency ranges can be correlated to physical processes (e.g. rainfall), and ratios of distinct ranges can be used to distinguish between weather patterns. Nystuen<sup>4</sup> used ratios of power levels at 5 and 25 kHz, although Quartly et al.<sup>3</sup> did not find good agreement with their own dataset. Some authors<sup>5</sup> used bands of 4-10 kHz vs. 10-30 kHz for rainfall analyses, but readily admitted the arbitrariness of the choice and concluded that "future work should examine other frequency bands for investigation". Our own analyses showed for example that, even if ratios of 4-10 vs. 10-30 kHz and 5 kHz vs. 25 kHz levels worked relatively well, a good separation between the different measurements could be seen using 5 kHz and 15 kHz levels (Figure 3).

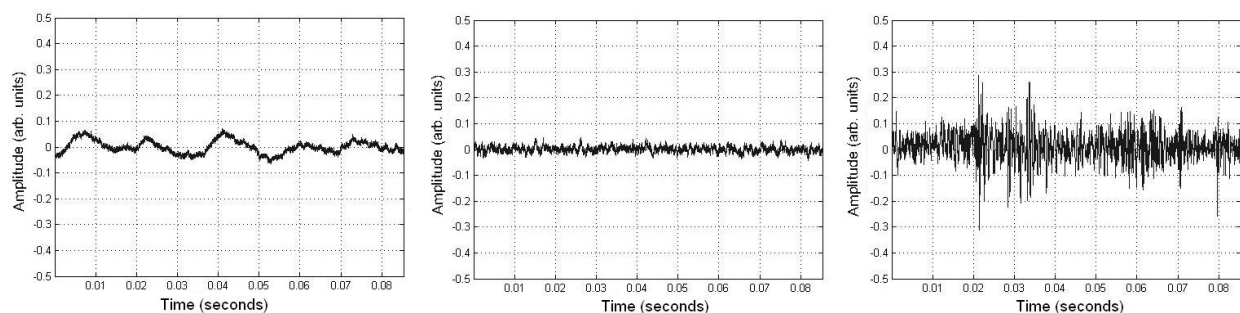


Figure 2: Example of raw files in time-domain: (left to right) recording stations A, C and E.

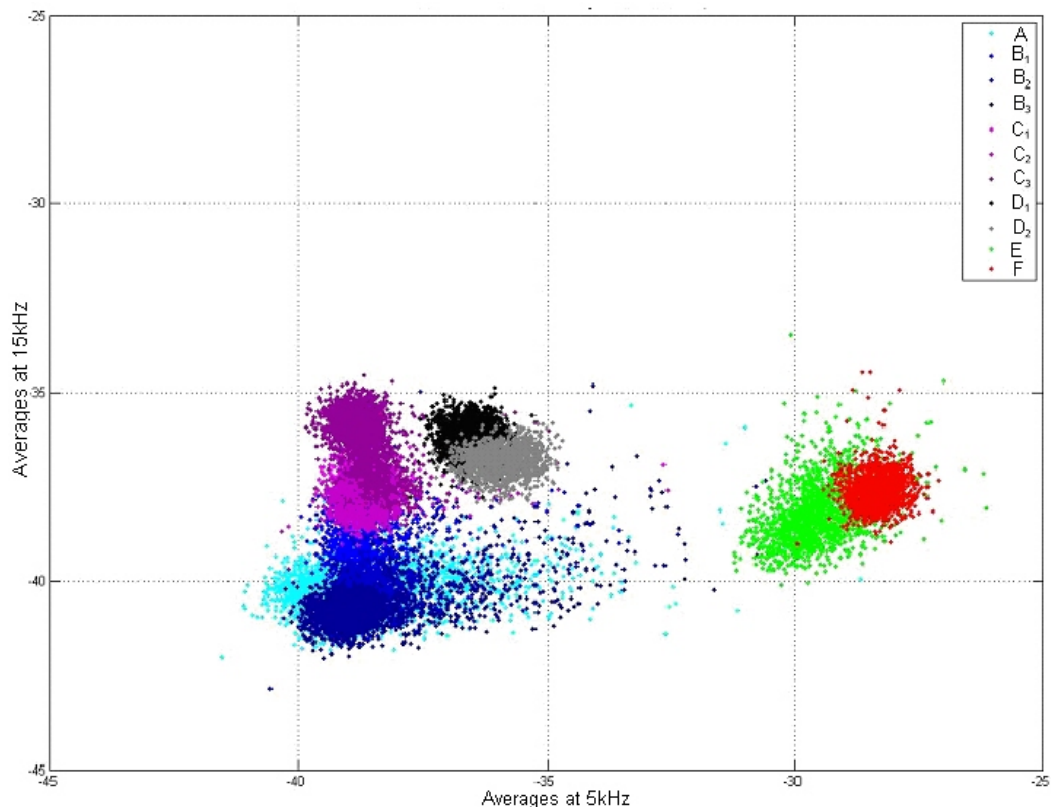


Figure 3: Acoustic classification of the Arctic measurements using averaged levels at 5 and 15 kHz. There is a clear distinction between recording stations, depending on environmental conditions (Table 1). But the choice of frequencies can be statistically refined (see text for details).

Following the recommendations of Black et al.<sup>5</sup>, we performed a more rigorous analysis by looking at the best combinations of frequency ranges to distinguish between measurements at the different recording stations. Principal Component Analysis, by maximising the variance between combinations of variables, could identify the most significant frequency bands. The results of this analysis are shown in figure 4. A large amount of the variance (91.6%) is accounted for by 3 discriminants, respectively labelled  $X_1$ ,  $X_2$  and  $X_3$ . Figure 4 also shows the frequency bands around which each of the discriminants are centred.  $X_1$  is centred on 5 kHz,  $X_2$  around 15 kHz and  $X_3$  around 45 kHz. This separation matches the physical processes at play according to experimental and theoretical studies<sup>4,5,9</sup>. Wind-related processes are going to influence mostly the frequencies in the calculation of  $X_1$ ; rain-related processes are predominant in the calculation of  $X_2$ , and  $X_3$  is a compound of low and (mostly) very high frequencies, more difficult to explain (and accounting for only 6% of the overall variance). The different measurements can be very well identified as distinct clusters (Figure 5). Variations in  $X_3$  are rather small, although at sites A, E and F, there are 'sub-clouds' with much lower values of  $X_3$ . These sub-clouds correspond to a small portion of the entire measurements. The sub-cloud in A presents regular variations along the  $X_3$  band, increasing and then decreasing linearly with time. Closer examination reveals potential contamination by the sonar of a passing vessel;  $X_3$  variations are consistent with the ship's track, local bathymetry and possible multipath propagation in the oceanographically complex conditions encountered at recording station A. The beginning of these measurements also sees marine mammal vocalisations (< 1 kHz), consistent with the behaviour of the whale observed at location A. The sub-cloud observed at recording station E shows combination of the lowest and highest frequencies (as per the definition of  $X_3$ ), and the role of the melting icebergs seems predominant. No definitive explanation can be provided for the sub-cloud in F, associated to a range of different factors (including noise from the berthing of a cruise ship in the harbour nearby). Overall, the separation along the  $X_1/X_2$  bands

perfectly matches the weather patterns observed at each recording station and their local variations (see Table 1).

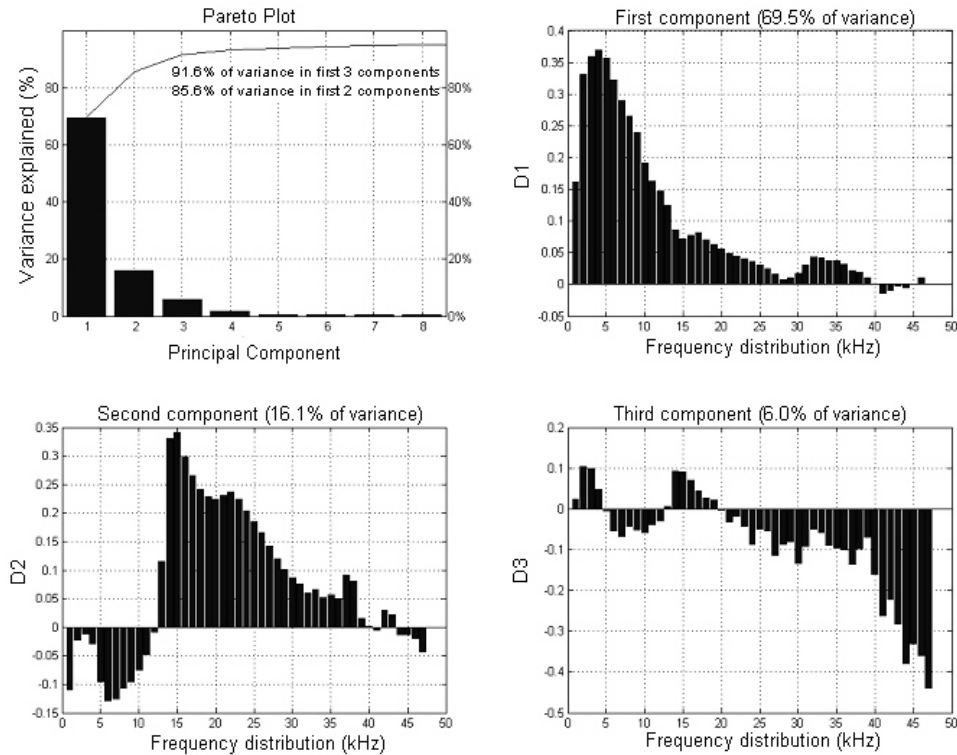


Figure 4: 3 frequency bands were identified through Principal-Component Analysis. Top left: contributions of each band to the total variance. Top right: band  $X_1$  corresponds to lower frequencies, centered on 5 kHz. Bottom left: band  $X_2$  encompasses medium frequencies (~15-30 kHz). Bottom right: band  $X_3$  mostly represents the highest frequencies measured.

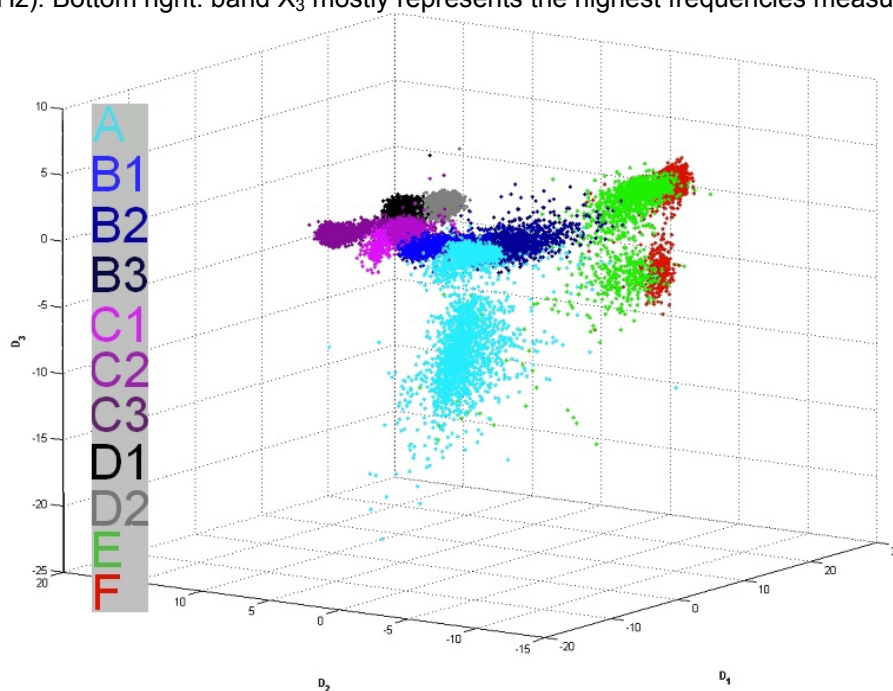


Figure 5: PCA plot of the three frequency ranges identified ( $X_1$ : lower frequencies,  $X_2$ : medium frequencies;  $X_3$ : mostly higher frequencies, with a small contribution from very low frequencies)



## 4 TANK EXPERIMENTS

Analysis of the Arctic measurements confirms the conclusions of previous studies. To better interpret our measurements and the combination of individual processes (e.g. wind and rain in a field of melting icebergs), laboratory experiments have been started to measure ambient noise in a fully controllable setting. The hydrophone used in the Arctic was set less than 1 m deep in the middle of a tank with dimensions 1.8 m x 1.2 x 1.2 m. Several weather-related processes were simulated. A large fan with variable settings simulated wind, and a hose simulated different types of rain. On its “cloud” setting, it produced a fine mist of small droplets, whereas its “spray” setting produced larger drop sizes. Rain rates could be varied and were measured each time (using a beaker). To simulate freshwater icebergs calving from the glacier, a 0.05-m<sup>3</sup> ice block was produced using the method of Barker and Timco<sup>10</sup>: frozen blocks of fresh water, ground to small pieces, were sieved and refrozen after addition of icy water, mimicking actual formation processes. Melting was recorded continuously and episodes of breaking/capsizing of sub-blocks identified acoustically and visually.

Frequencies could be sampled up to 44 kHz only in this setting. This prevented the full use of the three acoustic discriminants identified in the Principal Components Analysis of Section 3. Using the frequencies of Figure 3 (5 and 15 kHz respectively), the different processes can however be readily distinguished (Figure 6). Background noise (measured regularly throughout the experiment) corresponds to a very tight cluster of points. The melting of single ice blocks corresponds to another tight cluster, with lower levels (at least at these two frequencies): ice break-up events have a distinctive acoustic signature, and as the ice block melts further, the noise it generates logically merges with the background noise. The wind measurements and the two different types of rain produced with the hose are clearly distinguishable. Variations in the two rain measurement clusters are confidently attributed to variations in rain rate and raindrop sizes, in near-orthogonal directions.

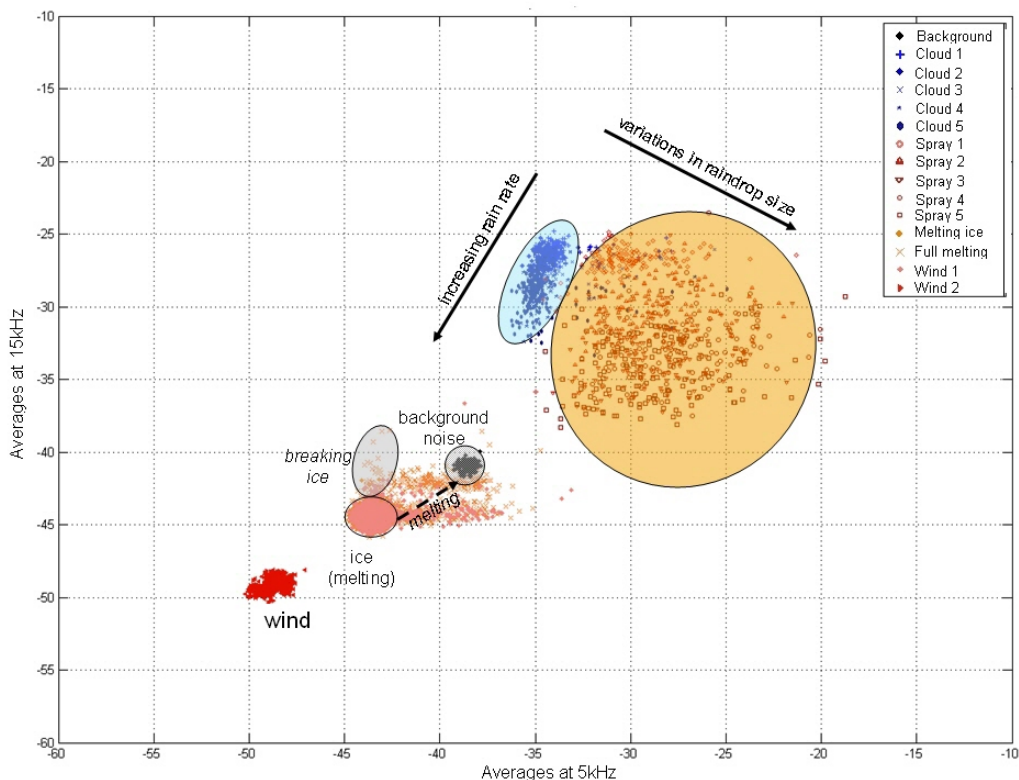


Figure 6: Acoustic classification of the tank measurements using averaged levels at 5 and 15 kHz (as in Figure 3). Individual processes can be clearly distinguished, including the melting of ice (with associated break-up and capsizing of sub-blocks) and variations in rainfall types.

## 5 DISCUSSION

The study of underwater acoustic noise generated by weather processes benefits from several decades of research and a large variety of applications<sup>1-5,9-11</sup>, although the work in Arctic fjords has been rather limited and mostly in Alaskan fjords<sup>12,13</sup>. The measurements presented here correspond to a single day of experiments, from a surface vessel, and therefore present a limited range of processes: small waves, wind, light rain, melting icebergs, marine mammals and passing ships. The wind was light, and rain rates did not vary significantly, remaining low. This range was however sufficient to justify the use of Principal-Component Analyses. The resulting frequency bands (Figure 4) confirm the current consensus about the main frequency characteristics of wind, rain and other processes. By looking at all frequencies, and not just the single values or narrow bands used in other studies, we were able to define more accurately and more rigorously the frequency bands typical of wind-related processes (band  $X_1$ ), rain-related processes (band  $X_2$ ) and mixed processes (band  $X_3$ ). Unexpected contributions to ambient noise underwater could also be detected and identified, such as the sonar from a ship further away and vocalisations from a minke whale. The field of melting icebergs can be clearly identified in the  $X_1/X_2/X_3$  space. These analyses (Figure 5) clearly match the surface observations of weather and other processes (Table 1). Distinct recordings made at the same location, a few minutes apart (e.g.  $C_1$ ,  $C_2$ ,  $C_3$ ) correspond to quasi-similar measurements, both in averaged frequency levels and in the PCA space, showing the good repeatability of this approach when the weather has not changed significantly.

A series of simple tank experiments was designed to check the acquisition system used in the Arctic, and to investigate the acoustic signatures of some of the processes observed, either individually or in combination. Due to space limitations, only a subset of these experiments is shown here. Its analysis supports previous conclusions, and matches those of other workers<sup>1-5,9-13</sup>. The current setup can however be improved in terms of accuracy and repeatability. Modulations in rain rate should be accompanied with measurements of raindrop size distributions, their velocity and their obliqueness, as all these parameters influence the acoustic measurements<sup>3-5,9,14</sup>. The observation of breaking and capsizing events did not include the volume and size of ice sub-blocks involved each time, and how they relate to the surges in ambient noise. Nonetheless, frequency analyses of the artificial events generated in the laboratory emphasize their acoustic differentiation (Figure 6). In the frequency range from 0.5 to 50 kHz, sounds generated by natural sources are mainly caused by physical processes at the ocean surface<sup>9</sup>. The distance over which they can be detected varies with frequency<sup>11</sup>. For the Arctic dataset, the hydrophone was ~9.5 m deep, yielding effective listening radii vary from 21.1 m (1 kHz) to 11.7 m (47 kHz). For the tank dataset, this varied from 2.4 m (at 1 kHz) to 1.5 m (at 22 kHz) respectively. Although potential echoes from tank walls would add to the overall signal, and its variability, laboratory-generated processes can be meaningfully compared to their real-world equivalents.

Comparison of field and laboratory measurements highlighted several issues for further studies. Arctic recordings were sampled at 96 kHz, enabling access to acoustic processes up to 48 Hz with good identification accuracy. Tank measurements, sampled at 44.1 kHz, enabled access to processes up to 22 kHz, and the successful distinction between processes would have benefited from access to higher frequencies to better compare with the field data. Frequency analyses should include suitable intervals below 1 kHz (for a better definition of noise from marine life, distant surf and shipping). Optimal sampling should encompass frequencies slightly higher than 80 kHz (limit imposed by thermal noise), as processes related to melting ice have been shown to encompass the entire frequency range<sup>15</sup>. Recording times should be of the order of minutes, as longer times are more likely to include weather changes (e.g. rainfall, wind speed) and shorter times might hamper the identification of other sources of noise (e.g. variations of ship noise with distance, correlation of marine mammal vocalisations with their visual observation). The resulting number of measurements with the same frequency signatures strengthens the identification of events. Finally, although good results could be obtained with a single hydrophone, the use of two hydrophones would have been useful to better identify the range and bearing of localised processes (e.g. passing vessel, rain squall, directivity of ice noise). This is now addressed in an on-going series of experiments.

## 6 SUMMARY

Ambient underwater noise can act as markers of weather patterns and human effects; it can also significantly affect sonar performance. Acoustic measurements of ambient noise were conducted in Kongsfjorden, Svalbard, in summer 2007. They were taken with a broadband hydrophone (100 Hz – 48 kHz effective bandwidth), deployed ~9.5-m deep at regular intervals from the mouth of the fjord toward the glaciers at its inner end. These measurements include ambient noise from wind and small waves, light rain, large ships, marine mammals and different types of freshwater growlers and bergy bits. Principal Component Analysis (PCA) of the frequency variations, averaged over 1-kHz bands, confirms and extends other studies in different environments. PCA results clearly distinguish weather patterns, the presence of icebergs and other contributions to ambient noise underwater. Laboratory experiments complement these observations and their interpretation. These field measurements are, to our knowledge, the first noise recordings taken in this environmentally significant region of the Arctic. They provide a first dataset on which to base analyses of the area's evolution with ocean weather patterns, climate change and anthropogenic activities.

## 7 ACKNOWLEDGEMENTS

The field survey was funded by the EC (grant ARCFAC-026129-70). MK is funded by an EPSRC Doctoral Training Award (# EPP5023061). J. Paine and M. White helped with the tank experiments.

## 8 REFERENCES

1. Wenz, G.M., *Acoustic ambient noise in the ocean: Spectra and sources*. J. Acoust. Soc. Am., 1962. **34**: p. 1936-1956.
2. Urick, R. J., *Principles of Underwater Sound*. 1975: McGraw Hill. 423.
3. Quartly, G.D., Gregory, J.W., Guymmer, T.H., Birch, K.G., Jones, D.W., Keogh, S.J., *How reliable are acoustic rain sensors?* Proc. Acoustical Oceanography, 2001: p. 142-148.
4. Nystuen, J.A., *Listening to raindrops from underwater: An acoustic disdrometer*. J. Atm. Ocean. Tech., 2001. **18**(10): p. 1640-1657.
5. Black, P.G., et al., *Oceanic rainfall detection and classification in tropical and subtropical mesoscale convective systems using underwater acoustic methods* Monthly Weather Review, 1997. **125**(9): p. 2014-2042.
6. Howe, J.A., et al., *Multibeam bathymetry and depositional environments of Kongsfjorden and Krossfjorden, western Spitsbergen, Svalbard*. Polar Res., 2003. **22**(2): p. 301-316.
7. Cottier, F., et al., *Water mass modification in an Arctic fjord through cross-shelf exchange: The seasonal hydrography of Kongsfjorden, Svalbard*. J. Geophys. Res., 2005. **110**.
8. Hop, H., et al., *The marine ecosystem of Kongsfjorden, Svalbard*. Polar Res., 2002. **21**: p. 167-208.
9. Ma, B.A., J.A. Nystuen, and R.-C. Lien, *Prediction of underwater sound levels from rain and wind*. Journal of Acoustical Society of America, 2005. **117**(6): p. 3555-3565.
10. Barker, A. and G. Timco, *Laboratory experiments of ice scour processes: rigid ice indenter*. Cold Regions Science and Technology, 2002. **35**: p. 196-206.
11. Farmer, D.M. and S. Vagle, *On the determination of breaking surface wave distributions using ambient sound*. J. Geophys. Res., 1988. **93**(C4): p. 3591-3600.
12. McConnell, S.O., M.P. Schilt, J.G. Dworski, *Ambient noise measurements from 100 Hz to 80 kHz in an Alaskan fjord*, J. Acoust. Soc. Am., 1992, **91**(4): p. 1990-2003.
13. NSWC (Naval Surface Warfare Center), *Glacier Bay Underwater Noise – August 2000 through August 2002*, NSWCCD-71-TR-2004/521, 2003, 78 pp.
14. Medwin, H., A. Kurgan and J.A. Nystuen, *Impact and bubble sound from raindrops at normal and oblique incidence*, J. Acoust. Soc. Am., **88**(1), 1990, p. 413-418.
15. Uscinski, B.J. and P. Wadhams, *Ice-ocean acoustic energy transfer: ambient noise in the ice-edge region*, Deep-Sea Res. II, **46**, 1999, p. 1319-1333.